Clays and Clay Minerals, Vol. 42, No. 1, 46–52, 1994.

REFINEMENT OF THE NACRITE STRUCTURE

HONG ZHENG AND STURGES W. BAILEY

Department of Geology and Geophysics, University of Wisconsin
1215 W. Dayton Street, Madison, Wisconsin 53706

Abstract—Nacrite crystals from a vug within a matrix of dickite at Red Mountain near Silverton, Colorado, have $a = 8.906(2)$, $b = 5.146(1)$, $c = 15.664(3)$ Å, $\beta = 113.58(3)°$, V = 657.9(3) Å^3, and space group *Cc*. The structure was solved by direct methods to determine phase angles, followed by electron density maps to locate all atoms. Refinement by least-squares ceased at R = 4.5%. Each 7 Å layer has structural detail very similar to those of dickite and kaolinite, although nacrite stacking is based on $-a/3$ interlayer shifts along the 8.9 Å axis (with octahedral cations alternating between the I and II sites in successive layers), whereas dickite and kaolinite are based on shifts of $-a/3$ along the 5.1 Å axis (with octahedral cations in the same set of sites in each layer). The angle of tetrahedral rotation is 7.8°, and the octahedral counter-rotations are 7.6° and 8.1°. The H^+ protons were located on DED maps. The inner O..H1 vector points exactly toward the vacant octahedron and is depressed −18.6° away from the level of the octahedral cations. All three surface OH groups have O...H vectors at 50° to 66° to (001), although OH2 may not participate in interlayer hydrogen bonding. All three interlayer OH–H–O contacts are bent to angles between 132° and 141° and form contacts between 2.94 and 3.12 Å. The interlayer separation of 2.915 Å is slightly larger than in dickite, interpreted as due to a less favorable meshing of the oxygen and hydroxyl surfaces in nacrite—a direct consequence of layer shifts along the 8.9 Å axis.

Key Words—Bond lengths, Crystal structure, Hydrogen bonds, Nacrite, Refinement, Tetrahedral rotation.

INTRODUCTION

Nacrite is the rarest of the kaolin polymorphs. Bailey and Tyler (1960) listed 16 occurrences known to them at that time, not all of which had been confirmed by X-ray study. Since then at least 20 additional occurrences, with X-ray confirmation, have been reported in the literature. Nacrite usually is considered as a high temperature kaolin polymorph, and most occurrences support a hydrothermal or pneumatolytic origin. Marumo (1989) collected oxygen isotope data that indicated increasing temperature of formation in the order kaolinite, dickite, nacrite, and pyrophyllite for clays in Kuroko deposits in northern Japan. Ushatinskiy *et al.* (1973) and Bühmann (1988); however, described nacrite in sediments, where an authigenic or low-temperature (<80°C) hydrothermal origin was postulated. Permyakov (1936) synthesized nacrite at 300°–335°C and 285–300 atmospheres. This is the only successful synthesis of nacrite known to us that has been confirmed by X-ray study of the product.

Hendricks (1939) was the first to determine the correct stacking of kaolin layers in nacrite. He used single crystals of nacrite from Pike's Peak, Colorado, to outline a six-layer cell with $c \simeq 43$ Å and approximate symmetry $R3c$. This meant that the atomic coordinates in the upper five layers could be derived from those of the first layer by operation of the rhombohedral symmetry elements. The actual symmetry was lowered to monoclinic *Cc* due to partial filling of the 18 general positions of $R3c$ by only 12 octahedral Al ions, and the cell was slightly distorted to give a β angle of 90°20′. The structure formed in this manner has the X and Y axes interchanged relative to their usual designations in layer silicates, and every layer is shifted by $a/3$ in the same direction (+ or −) along the 8.9 Å repeat. Every other layer is rotated by 180°. Hendricks pointed out that the layers were bonded across the interlayer space by "hydroxyl bonds" (now termed long hydrogen bonds) in which surface OH groups paired closely with basal oxygens of the next layer, and he emphasized the importance of such bonding in the polymorphism of the kaolin minerals. This structure is quite different from the four-layer structure with $\beta = 91°43'$ proposed by Gruner (1933) for nacrite from Brand, Saxony, on the basis of X-ray powder data. Gruner recognized the 180° rotation of alternate layers, but not the interchange of the X and Y axes.

Newnham (1961) recognized that there were only two different kinds of layers in the Hendricks' structure of nacrite and that it could be described as a two-layer structure with a larger β angle of 100°. He derived 36 ways to superimpose two kaolin layers to give long interlayer hydrogen bonds; 12 of these assemblages have the least cation-cation repulsion across the interlayer space. But the two-layer structures of dickite and nacrite were judged the most stable because they were the only ones in which the grooves and ridges of the layer surfaces due to dioctahedral distortions would mesh across the interlayer space. Kaolinite has a less favorable interface between layers. Radoslovich (1963) pointed out that the dickite structure should be more stable than that of nacrite because it minimizes the

angular strain on each of the three directed interlayer O...H vectors, which ideally should be coplanar with the two closest Al^{3+} cation neighbors. In nacrite only one of the basal oxygens (03) is located so it can pair up ideally with a directed hydrogen bond of this type. The other two basal oxygens (01 and 02) are located so that the actual bonds must be nearly at right angles to the ideal directed bonds, and this must affect the nacrite stability adversely. This difference in geometry of the O–OH bonds is due to the difference in the interlayer shift directions (along the 5.1 Å axis in dickite and along the 8.9 Å axis in nacrite).

Bailey (1963) confirmed the validity of the two-layer structure of nacrite and recommended using a β angle of ~114° so that $+Z$ points in the same direction in plan view as the interlayer shifts. The sequence of layers is that of the standard $6R$ polytype (later designated $6R_1$) derived by Bailey (1969) for trioctahedral 1:1 layer silicates. The octahedral vacancy alternates in adjacent layers between the B and C sites on opposite sides of the pseudo-mirror plane of each layer, taking into account the 180° rotation of alternate layers (equivalent to alternate occupation of the I and II sets of possible octahedral sites). It is this ordered pattern of octahedral cations and vacancies that reduces the symmetry from the ideal rhombohedral $R3c$ to monoclinic Cc and allows choice of a smaller two-layer cell.

Blount *et al.* (1969) made the first refinement of the two-layer structure of nacrite, using the Weissenberg film technique on crystals from Pike's Peak, Colorado. Complete refinement was inhibited (R = 10%) because of the presence of out-of-step domains in which the interlayer shifts were in the wrong direction ($+a/3$ instead of $-a/3$). Zvyagin *et al.* (1972) also refined the structure (R = 12%) using high-voltage electron diffraction in the oblique texture mode on fine-grained nacrite from the western Transbaikal region of the U.S.S.R. Their structure differed slightly from that of Blount *et al.* (1969) in the coordinates of several atoms and, more importantly, in a smaller tetrahedral rotation angle of 3.2° relative to 7.3°. They attributed the smaller angle to the counterattraction of the basal oxygens by octahedral cations in the adjacent layer.

This paper reports a new refinement of nacrite using an automated single-crystal X-ray diffractometer. The purposes of the study were to achieve higher accuracy in atomic coordinates so that the discrepancies between the two previous refinements could be resolved and, if possible, to locate H^+ protons associated with the OH groups. The nacrite used was from a previously unreported occurrence within vugs of a hydrothermal dickite deposit at Red Mountain near Silverton, Colorado. Interlocking boxworks of thin nacrite platelets 0.1 to 1.0 mm in diameter within small cavities of a dickite matrix were found in two separate micromounts in the G. L. English collection (University of Wisconsin Geology Museum #U.W. 6003/1 and U.W. 6003/2).

EXPERIMENTAL METHODS

An approximately triangular section 0.6 × 0.5 × 0.5 mm on the sides and 0.01 mm thick was cut from a larger crystal taken from specimen UW #6003/1 and used to collect intensity data on a Siemens P4 rotating anode single-crystal diffractometer. The crystal used showed sharp optical extinction and no visible twinning. The diffraction spots were slightly diffuse but were not streaked. Data were collected using the β = 100° cell, but all results reported here were transformed to the preferred β = 114° cell of Bailey (1963), and the atom designations are the same as those of Blount *et al.* (1969). The transformed unit cell parameters are a = 8.906(2), b = 5.146(1), c = 15.664(3) Å, β = 113.58(3)°, and V = 657.9(3) Å^3, obtained by centering 12 medium-angle reflections (2θ = 45° to 57°, MoKα radiation). These values give $c \sin\beta$ = 14.356 Å. A more accurate value of $c \sin\beta$ = 14.364(1) Å was obtained by extrapolating the absorption function to θ = 90° for values of $\ell d(00\ell)$ from ℓ = 16 to 18 (θ = 59° to 75° with CuKα_1 X-radiation) as measured from a film pattern from the same crystal mounted in a Debye-Scherrer camera of 114.6 mm diameter.

A total of 3890 reflections was collected in all octants out to 2θ = 60° with monochromatic MoKα radiation. A θ–2θ scan technique was used with a scan width of 2.2° 2θ and variable scanning speeds from 2° to 30° per minute. Two standard reflections were checked every 100 reflections to monitor the crystal and electronic stability. No instability was found. The data were corrected for the Lp factor and for absorption using both the semi-empirical psi-scan technique and an analytical shape correction, then merged into 827 monoclinic reflections.

REFINEMENT

Initial atomic coordinates were determined by direct methods using program SHELXTL for phase angle determination, followed by electron density maps to locate all of the atoms. These atomic coordinates confirmed the 2-layer structure of Blount *et al.* (1969) and gave an initial residual R of 23.5%.

Because of the thinness of the crystal, refinement was attempted with data sets in which absorption was taken into account in three different ways: 1) empirical psi-scan correction, 2) theoretical analytical shape correction, and 3) no absorption correction, but with 30 low-angle reflections most apt to be affected by absorption removed from the data set. Each data set was refined, and the thermal ellipsoids were plotted by program ORTEP. The ellipsoids for the two data sets without absorption correction and as corrected by psi-scan were markedly more elongate parallel to Z^* than for the data set corrected by the analytical shape correction. Because residual absorption effects were suspected even in the latter data set because of past experience with

Table 1. Final atomic parameters.

Atom	x	y	z	β_{11}	β_{22}	β_{33}	β_{12}	β_{13}	β_{23}
Al(1)	0.1552(3)	0.3198(4)	0.2177(2)	0.0034(3)	0.0090(7)	0.0017(1)	0.0000(3)	0.0012(1)	−0.0002(2)
Al(2)	0.4901	0.3245(4)	0.2173	0.0033(3)	0.0082(8)	0.0021(1)	−0.0003(3)	0.0016(1)	−0.0002(2)
Si(1)	0.2012(3)	0.4700(4)	0.0277(2)	0.0034(3)	0.0052(7)	0.0021(1)	−0.0001(3)	0.0016(1)	0.0000(2)
Si(2)	0.3715(3)	0.9831(4)	0.0270(2)	0.0036(3)	0.0065(7)	0.0017(1)	−0.0002(3)	0.0013(1)	−0.0001(2)
O(1)	0.2411(6)	0.7499(10)	−0.0041(4)	0.0047(7)	0.0097(18)	0.0023(2)	0.0028(8)	0.0014(3)	0.0005(5)
O(2)	0.2723(6)	0.2470(10)	−0.0188(4)	0.0053(7)	0.0080(16)	0.0023(2)	−0.0013(8)	0.0019(3)	0.0000(5)
O(3)	0.0029(6)	0.4417(10)	−0.0193(3)	0.0034(6)	0.0124(18)	0.0019(2)	−0.0004(8)	0.0012(3)	0.0003(5)
O(4)*	0.2696(6)	0.4385(9)	0.1385(4)	0.0021(5)	0.0047(14)	0.0024(2)	−0.0004(7)	0.0014(3)	−0.0001(5)
O(5)*	0.4618(6)	0.0110(10)	0.1381(4)	0.0040(6)	0.0115(18)	0.0020(2)	−0.0026(8)	0.0014(3)	0.0004(5)
OH(1)	0.0795(6)	0.0118(10)	0.1432(4)	0.0053(7)	0.0095(18)	0.0023(2)	0.0024(8)	0.0021(3)	0.0006(5)
OH(2)	0.5580(6)	0.6342(10)	0.2838(4)	0.0054(7)	0.0118(18)	0.0020(2)	−0.0016(8)	0.0018(3)	0.0000(5)
OH(3)	0.1780(6)	0.6296(10)	0.2825(4)	0.0043(6)	0.0099(17)	0.0019(2)	0.0007(8)	0.0012(3)	0.0000(5)
OH(4)	0.3693(7)	0.2066(11)	0.2826(4)	0.0049(6)	0.0154(19)	0.0016(2)	−0.0010(9)	0.0013(3)	−0.0010(5)
H(1)	0.6346	0.4510	0.1277						
H(2)	0.5475	0.6736	0.3279						
H(3)	0.2432	0.6096	0.3296						
H(4)	0.4317	0.1386	0.3228						

* = apical oxygen.
Numbers in parentheses represent one standard deviation of the last decimal place.

difficulty in measuring the thickness of very thin crystals, 30 low-angle reflections were removed from the latter data set for a final refinement. Only results from the latter refinement are reported here, but it should be noted that the differences in the resulting atomic coordinates and bond lengths for the three refinements are small—always in the last decimal place reported. The differences are in the shapes of the thermal ellipsoids and to a lesser degree in the standard deviations of atomic coordinates.

During refinement the x and z coordinates of atom Aℓ2 were held constant while all other parameters were varied using a modified version of the least-squares program ORFLS. Unit weights and half-ionized scattering factors were used throughout. Isotropic temperature factors were used until R declined to 7.9% and then changed to anisotropic factors. When refinement ceased, difference electron density (DED) maps were flat at all atomic positions. The scattering contributions of hydrogen are mainly to the low-angle reflections, so the 30 reflections deleted during refinement of the non-hydrogen atoms were returned to the data set in an attempt to locate the H^+ protons on DED sections. Small positive anomalies of 0.3 to 0.4 electrons were found near the OH groups, which were taken as the positions of the H^+ protons. These positions did not change when the 30 reflections were removed from the data set as a check. For comparison purposes, 0.08 e/Å^3 corresponds to the background value averaged over the 480 independent points of one DED section chosen to be away from any atomic position. The final residual R of 4.5% incorporates these H^+ positions, which were not refined.

Table 1 lists the final atomic parameters, and Table 2 lists the orientations of the thermal ellipsoids. Table 3 gives calculated bond lengths and angles from program ORFFE. Table 4 lists selected structural features of nacrite.

DISCUSSION

The bond lengths and angles reported in Table 3 and the structural features reported in Table 4 are in much better agreement with those of dickite and other layer silicate structures than given by either the refinements of Blount *et al.* (1969) or Zvyagin *et al.* (1972). The atomic coordinates cannot be compared directly with those of the previous authors because x and z of A12 were held constant at the values given by the initial electron density map rather than at either set of prior published values.

The calculated tetrahedral rotation angle of 7.8° compares well with the 7.3° angle given for nacrite by Blount *et al.* (1960), but is substantially larger than the 3.2° angle of Zvyagin *et al.* (1972). The structural details of each 7 Å layer are very similar to those of the most recent refinements of dickite and kaolinite, as summarized by Giese (1988). The octahedral cations

are closer to the upper OH plane than to the lower O,OH plane, and the upper and lower anion triads of the octahedra are counterrotated by 7.6° and 8.1°, respectively, as a consequence of shortening of shared edges. The shared diagonal octahedral edges around A11 and A12 average 2.383 Å *vs.* 2.845 Å for unshared diagonal edges and 2.781 Å for the lateral edges. The lateral edges around the vacant octahedron average 3.409 Å. The tetrahedra are tilted because of these latter large edges, elevating basal oxygen 01 by 0.215 Å above the level of 02 and 03. This elevated 01 is paired with an elevated OH2 across the interlayer space, but the three surface OH groups are more nearly coplanar than in dickite. It should be noted that the OH2-01 separation is the largest of the three interlayer bond contacts (Table 3), and the participation of OH2 in hydrogen bonding is controversial.

Zheng and Bailey (1989) compared the results of locating H^+ protons in chlorites by X-ray diffraction using DED maps relative to the more accurate neutron diffraction method. They concluded that, in some cases, the X-ray results are within 0.05 to 0.10 Å of the neutron results, but, in other cases, the excess electron densities are probably artifacts. In the present study of nacrite, the O..H distances determined within the four hydroxyls are between 0.70 and 0.76 Å, which are shorter than the generally accepted values (0.95 to 1.0 Å). The three surface hydroxyls have H..O interlayer contacts between 2.331 and 2.535 Å; their OH–H–O angles are between 132° and 141°; and their contacts with the basal oxygens are between 2.944 and 3.117 Å (Table 3). The O..H bonds from the surface hydroxyls are oriented between 50° to 66° from the (001) plane, whereas O..H from the inner hydroxyl points exactly towards the vacant octahedron in plan view but is depressed 18.6° away from the octahedral sheet into the tetrahedral sheet.

Figure 1 shows the projections onto (001) of the H^+ positions for nacrite as determined in this study relative to the theoretical positions determined by Giese and Datta (1973) by minimization of the total electrostatic energy using the non-hydrogen atomic positions of Blount *et al.* (1969). The experimental points in projection all lie about 0.35 Å from the theoretical points. Much of this difference is due to the O...H distances of 0.70 to 0.76° Å found within each hydroxyl in this study instead of the more realistic value of 0.97 Å used by Giese and Datta for their calculations. These shorter distances automatically increase the H–O distances to the acceptor oxygens and increase the OH–H–O angles.

Giese and Datta (1973) believed OH2 did not participate in interlayer hydrogen bonding in nacrite because 1) the O...H2 vector from OH2 was calculated to have minimum electrostatic energy when oriented at 38° to (001) relative to values of 79° and 73° calculated for O...H3 and O...H4, respectively; 2) the calculated H2-01 distance of 2.60 Å was just equal to the sum of the van der Waals radii of hydrogen and oxygen and considerably larger than the 2.02 Å distance calculated for the other two H–O contacts; and 3) the point involving OH2 on a plot of the two Al–OH–H angles *vs.* one another fell on the 45° line indicating equality of the angles and, thus, non bonding. The authors state that the two Al–OH–H angles hypothetically should be equal unless there are outside influences, such as hydrogen bonding. Giese (1973) later concluded that H2 makes a very small contribution to the interlayer bonding on the basis of a small decrease in slope of a plot of Coulomb energy *vs.* interlayer distance when OH2 is replaced by F in the calculations. It should be noted that the theoretical minimum energy positions for the H^+ protons undoubtedly would change somewhat if calculated on the basis of the more accurate non-hydrogen atomic positions determined in the present study.

Table 2. Shape and orientation of thermal ellipsoids.

Atom	Axis	RMS displacement (Å)	Angles with respect to		
			X	*Y*	*Z*
Al(1)	R1	0.102(5)	169(14)	79(14)	65(6)
	R2	0.110(5)	79(14)	14(2)	88(12)
	R3	0.133(4)	90(6)	82(7)	155(6)
Al(2)	R1	0.091(5)	171(12)	99(13)	64(4)
	R2	0.105(5)	99(13)	10(2)	83(7)
	R3	0.147(4)	94(3)	86(4)	153(3)
Si(1)	R1	0.084(5)	99(10)	171(20)	86(9)
	R2	0.093(5)	10(1)	99(20)	117(4)
	R3	0.147(3)	94(3)	90(2)	153(3)
Si(2)	R1	0.093(5)	97(6)	173(16)	88(8)
	R2	0.104(4)	8(5)	97(16)	117(5)
	R3	0.135(3)	93(5)	88(4)	153(5)
O(1)	R1	0.091(11)	127(8)	39(4)	84(6)
	R2	0.142(8)	38(6)	52(9)	108(24)
	R3	0.156(8)	84(9)	97(16)	161(23)
O(2)	R1	0.095(11)	117(12)	153(12)	77(8)
	R2	0.130(8)	151(21)	63(11)	60(9)
	R3	0.157(7)	100(12)	89(8)	147(12)
O(3)	R1	0.102(9)	167(14)	102(16)	71(10)
	R2	0.128(9)	99(17)	25(5)	107(26)
	R3	0.142(8)	81(10)	112(16)	154(20)
O(4)	R1	0.067(13)	157(16)	112(17)	72(6)
	R2	0.082(12)	113(17)	23(7)	82(13)
	R3	0.158(7)	86(4)	90(5)	161(4)
O(5)	R1	0.083(12)	141(7)	129(7)	69(6)
	R2	0.140(8)	61(8)	122(17)	63(13)
	R3	0.149(8)	66(7)	125(17)	145(32)
OH(1)	R1	0.095(11)	131(12)	41(12)	74(10)
	R2	0.127(9)	133(13)	126(3)	48(11)
	R3	0.160(7)	109(9)	106(9)	134(10)
OH(2)	R1	0.108(10)	42.3(9)	50(15)	118(12)
	R2	0.135(9)	121(18)	43(7)	52(13)
	R3	0.150(8)	115(17)	76(21)	129(21)
OH(3)	R1	0.109(10)	127(17)	38(8)	79(12)
	R2	0.124(9)	39(8)	53(8)	99(21)
	R3	0.142(8)	80(17)	87(16)	166(16)
OH(4)	R1	0.119(9)	58(16)	113(28)	155(12)
	R2	0.125(9)	34(5)	66(17)	89(22)
	R3	0.152(9)	99(14)	34(5)	115(12)

https://doi.org/10.1346/CCMN.1994.0420106 Published online by Cambridge University Press

Table 3. Bond lengths (Å) and angles (°).

Si1–O1	1.610(5)	O1–O2	2.623(8)	O1-Si1-O2	108.7(3)
O2	1.617(5)	O1–O3	2.583(7)	O1 O3	105.9(3)
O3	1.626(5)	O1–O4	2.678(7)	O2 O3	106.4(3)
O4*	1.601(5)	O2–O3	2.597(7)	O1 O4	113.0(3)
Mean	1.613(2)	O2–O4	2.662(7)	O2 O4	111.6(3)
		O3–O4	2.657(6)	O3 O4	110.8(2)
		Mean	2.633(3)	Mean	109.4(1)
Si2–O1	1.604(5)	O1–O2	2.593(8)	O1-Si2-O2	107.0(3)
O2	1.622(5)	O1–O3	2.629(6)	O1 O3	109.3(8)
O3	1.618(5)	O1–O5	2.670(7)	O2 O3	106.0(3)
O5*	1.605(5)	O2–O3	2.583(7)	O1 O5	112.6(3)
Mean	1.612(2)	O2–O5	2.654(7)	O2 O5	110.6(3)
		O3–O5	2.658(7)	O3 O5	111.1(2)
		Mean	2.631(3)	Mean	109.4(1)
		Lateral edges		Diagonal edges	
Al1–O4	1.991(5)	O4–O5	2.764(6)	Shared	
O5	1.942(5)	O4–OH1	2.792(7)	O4–OH4	2.389(7)×2
OH1	1.923(6)	O5–OH1	2.763(8)	O5–OH3	2.390(7)×2
OH2	1.858(5)	OH2–OH3	2.768(8)	OH1–OH2	2.371(7)×2
OH3	1.857(6)	OH2–OH4	2.804(7)	Mean	2.383(4)
OH4	1.860(6)	OH3–OH4	2.763(8)	Unshared	
Mean	1.905(2)	Mean	2.778(3)	O4–OH3	2.862(7)×2
				O5–OH2	2.853(7)×2
				OH1–OH4	2.816(7)×2
				Mean	2.844(4)
Al2–O4	1.945(5)	O4–O5	2.789(6)	Shared	
O5	1.989(5)	O4–OH1	2.758(6)	O4–OH4	2.389(7)×2
OH1	1.912(5)	O5–OH1	2.772(8)	O5–OH3	2.390(7)×2
OH2	1.867(5)	OH2–OH3	2.811(8)	OH1–OH2	2.371(7)×2
OH3	1.866(5)	OH2–OH4	2.765(8)	Mean	2.383(4)
OH4	1.859(5)	OH3–OH4	2.779(7)	Unshared	
Mean	1.906(2)	Mean	2.784(3)	O4–OH2	2.849(7)×2
				O5–OH4	2.883(7)×2
				OH1–OH3	2.806(8)×2
				Mean	2.846(4)

Vacant octahedron lateral edges		Angles Al-OH-H		
			Al1	Al2
O4–O5	3.409(7)	H1	117.0	120.3
O4–OH1	3.417(7)	H2	128.6	127.1
O5–OH1	3.438(7)	H3	107.2	142.5
OH2–OH3	3.377(6)	H4	150.5	102.6
OH2–OH4	3.387(8)			
OH3–OH4	3.423(8)			
Mean	3.409(3)			

Interlayer contacts		Hydrogen distances		Hydrogen angles	
O1–OH2	3.117(7)	OH1..H1	0.70(6)	OH2-H2-O1	135(3)
O2–OH3	2.951(7)	OH2..H2	0.76(12)	OH3-H3-O2	132(4)
O3–OH4	2.944(7)	H2--O1	2.535(10)	OH4-H4-O3	141(6)
Mean	3.004(4)	OH3..H3	0.74(10)		
		H3--O2	2.400(11)	Angle O..H to (001)	
		OH4..H4	0.74(8)	H1	−18.6
		H4--O3	2.331(6)	H2	56.8
				H3	65.9
				H4	50.3

In the present study the experimental position found for H2 is such that the angle of O...H2 to (001) increases from the 38° value of Giese and Datta (1973) to 57° (which makes A11, A12, OH2, and H2 almost exactly coplanar), and the H2-01 distance decreases to 2.535 Å (it would be even shorter if the O...H2 distance were 0.97 Å instead of 0.76 Å). The two experimental A1–OH2–H2 angles are nearly equal, however, in support of the theoretical values of Giese and Datta (1973). The O...H3 vector found in the present study is tilted

https://doi.org/10.1346/CCMN.1994.0420106 Published online by Cambridge University Press

Table 4. Other important structural features.

Parameter	Site	Value
Octahedral distortion RMS (15)	Al(1)	9.45
	Al(2)	9.43
Octahedral distortion RMS (36)	Al(1)	5.74
	Al(2)	5.80
Octahedral rotation (°)	upper triad	7.62
	lower triad	8.13
Octahedral flattening Ψ_{oct} (°)	Al(1)	57.4
	Al(2)	57.4
Tetrahedral angle τ (°)	Si(1)	111.8
	Si(2)	111.4
Tetrahedral rotation α_{tet} (°)		7.76
Basal oxygen Δz (Å)		0.215
Sheet thickness (Å)		
Tetrahedral		2.212
Octahedral		2.055
Interlayer separation (Å)		2.915
Interlayer shift		$-0.353a_1$
β_{ideal} (°)		112.28

away from acceptor oxygen 02, which is unrealistic. Experimental point H4 is also unrealistic in that it deviates in plan view (Figure 1) from a straight line between OH4 and 03. The points for OH3 and OH4, however, both lie well within the fields of hydrogen bonding in the Al–OH–H angle plot. The O...H1 vector is depressed 18.6° below the octahedral sheet and appears to point in the expected direction (Figure 1), although the O...H1 distance is shorter than expected. The two Al–OH1–H1 angles are nearly equal (Table 3).

In summary, the positions for the H^+ protons found in this study differ from the theoretical minimum energy positions because of the short O...H distances found and the deviations of H3 and H4 from the expected geometry for hydrogen bonds. The peaks interpreted as H^+ positions were the only extra DED peaks near the OH groups. The e/Å^3 values of the peaks were H1 = 0.38, H2 = 0.30, H3 = 0.34, and H4 = 0.40. These values range from 3.75σ to 5.0σ, using the average background value of 0.08 for σ. If the equation of Ladd and Palmer (1977, p. 292) is used to calculate the DED background, then $\sigma(\rho_0) = 0.05$, and the H^+ peaks range from 6.0σ to 8.0σ. But these tests only indicate that the extra DED peaks are significantly above background, not that they necessarily represent the true positions of the H^+ protons. The presence of systematic absorption errors in the data is suspected because of the unrealistic thermal ellipsoids of the atoms (see below).

A neutron diffraction refinement is needed to determine the correct positions of the H^+ protons. The H^+ positions as determined in the present study, however, do support the views of Giese and Datta (1973) and Giese (1973) that OH2 does not participate appreciably in interlayer hydrogen bonding. The average interlayer separation of 2.915 Å (Table 4) is slightly larger than found in dickite (2.883 to 2.887 Å), leading to a slightly larger d(001). This is interpreted as due to a less favorable meshing of the oxygen and hydroxyl surfaces in nacrite resulting from the positions of OH2 and OH3 relative to 01 and 02—a direct consequence of layer shifts along the 8.9 Å axis.

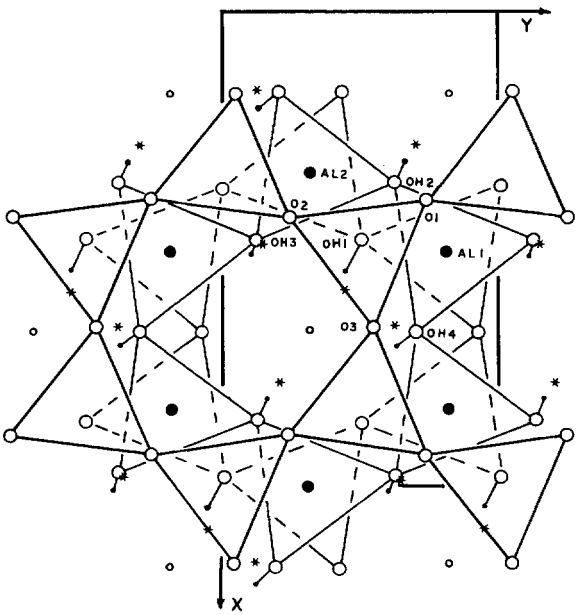

Figure 1. Projection onto (001) of basal oxygens in the tetrahedral sheet of the second layer onto the octahedral sheet of the first layer. Small solid circles are H^+ positions found in this study. Small asterisks are theoretical H^+ positions calculated by Giese and Datta (1973). Small open circles are centers of the vacant octahedra.

None of the thermal β_{ij} values proved to be nonpositive definite during refinement, but they are not believed to represent true thermal motion. For phyllosilicates the bridging tetrahedral basal oxygens should vibrate normal to the Si–O–Si bond. Table 2 shows this is not the case for the present refinement. The major axes of the thermal ellipsoids for the basal oxygens instead are essentially normal to the layer. Similar results have been noted in other refinements of layer structures involving very thin platelets.

ACKNOWLEDGMENTS

This research was supported in part by National Science Foundation grant EAR-8614868 and in part by grant 17966-AC2-C from the Petroleum Research Fund, administered by the American Chemical Society. We are indebted to the Department of Chemistry, University of Wisconsin–Madison, for use of their diffraction facilities and to Randy Hayashi for technical assistance.

REFERENCES

Bailey, S. W. (1963) Polymorphism of the kaolin minerals: *Amer. Mineral.* **48,** 1196–1209.

Bailey, S. W. (1969) Polytypism of trioctahedral 1:1 layer silicates: *Clays & Clay Minerals* **17,** 355–371.

Bailey, S. W. and Tyler, S. A. (1960) Clay minerals associated with the Lake Superior iron ores: *Econ. Geol.* **55,** 150–175.

Blount, A. M., Threadgold, I. M., and Bailey, S. W. (1969) Refinement of the crystal structure of nacrite: *Clays & Clay Minerals* **17,** 185–194.

Bühmann, D. (1988) An occurrence of authigenic nacrite: *Clays & Clay Minerals* **36,** 137–140.

Giese Jr, R. F. (1973) Interlayer bonding in kaolinite, dickite and nacrite: *Clays & Clay Minerals* **21,** 145–149.

Giese Jr., R. F. (1988) Kaolin minerals: Structures and stabilities: Chapter 3 in *Hydrous Phyllosilicates (Exclusive of Micas)*, S. W. Bailey, ed., *Reviews in Mineralogy* **19,** Mineralogical Society of America, Washington, D.C., 29–66.

Giese Jr, R. F. and Datta, P. (1973) Hydroxyl orientation in kaolinite, dickite, and nacrite: *Amer. Mineral.* **58,** 471–479.

Gruner, J. (1933) The crystal structure of nacrite and a comparison of certain optical properties of the kaolin group with its structures: *Zeit. Kristallogr.* **85,** 345–354.

Hendricks, S. B. (1939) The crystal structure of nacrite $Al_2O_3 \cdot 2SiO_2 \cdot 2H_2O$ and the polymorphism of the kaolin minerals: *Zeit. Kristallogr.* **100,** 509–518.

Ladd, M. F. C. and Palmer, R. A. (1977) *Structure Determination by X-ray Crystallography:* Plenum, New York, 393 pp.

Marumo, K. (1989) Genesis of kaolin minerals and pyrophyllite in Kuroko deposits of Japan: Implications for the origins of the hydrothermal fluids from mineralogical and stable isotope data: *Geochim. Cosmochim. Acta* **53,** 2915–2924.

Newnham, R. E. (1961) A refinement of the dickite structure and some remarks on polymorphism in kaolin minerals: *Mineral. Mag.* **32,** 683–704.

Permyakov, V. M. (1936) Über hydrothermale Synthese des Kaolins (in Russian): *Acad. Sci. USSR, Vernadsky Jubilee Vol.,* 563–580.

Radoslovich, E. W. (1963) The cell dimensions and symmetry of layer-lattice silicates. IV. Interatomic forces: *Amer. Mineral.* **48,** 76–99.

Ushatinskiy, I. N., Babitsyn, P. K., and Kiesleva, F. P. (1973) Dickite and nacrite in Mesozoic deposits of western Siberia: *Akad. Nauk SSSR, Doklady Earth Sci. Section* **209,** 107–109.

Zheng, H. and Bailey, S. W. (1989) Structures of intergrown triclinic and monoclinic II*b* chlorites from Kenya: *Clays & Clay Minerals* **37,** 308–316.

Zvyagin, B. B., Soboleva, S. V., and Fedotov, A. F. (1972) Refinement of the structure of nacrite by high-voltage electron diffraction: *Soviet Phys. Crystall.* **17,** 448–452.

(Received 21 June 1993; accepted 6 October 1993; Ms. 2386)